A Backstepping based Controller utilizing a Sliding Mode Disturbance Observer Applied to Hydraulic Servo Systems

Manganas, Ioannis; Schmidt, Lasse; Andersen, Torben Ole; Pedersen, Henrik C.

Published in:
Modeling, Identification and Control (Online)

DOI (link to publication from Publisher):
10.4173/mic.2023.1.3

Publication date:
2023

Document Version
Publisher's PDF, also known as Version of record

Modeling, Identification and Control, Vol. 44, No. 1, 2023, pp. 31–42, ISSN 1890–1328

A Backstepping based Controller utilizing a Sliding Mode Disturbance Observer Applied to Hydraulic Servo Systems

I. Manganas [2] L. Schmidt [1] T. O. Andersen [1] H. C. Pedersen [1]

[1] *Fluid Power and Mechatronic Systems, Department of Energy Technology, Aalborg University, Pontoppidanstraede 111, 9220 Aalborg, Denmark. E-mail:* {lsc, toa, hcp}@energy.aau.dk

E-mail: manganas.ioannis@gmail.com

Abstract

Hydraulic servo systems are characterized by nonlinear dynamics that can render control design challenges. Controllers for a linearized model will typically be conservative, and the stability of the closed loop system, in the Lyapunov sense, may be difficult to prove. On the contrary, the backstepping technique can lead to control algorithms for which stability margins can be estimated. However, these tend to be complex algorithms that are difficult to apply. In this paper, the backstepping control design procedure is applied to a hydraulically actuated robot. A sliding mode disturbance observer is utilized to avoid the high complexity of the backstepping algorithm. The paper's primary focus is hence on proving the stability of the proposed algorithm and its applicability to a laboratory setup. However, ways to improve performance are also discussed. Finally, results are presented where the designed controller is tested in both simulations and applied to the laboratory setup, and compared to linear controllers.

Keywords: Hydraulics, Backstepping Control, Nonlinear, Servo System

1 Introduction

Electric drive systems are almost ubiquitous in low-power systems. On the other hand, for high-power applications, using a gearbox is unavoidable. However, the gearbox introduces backlash and increased maintenance costs. As a result, hydraulic drive systems can substitute their electrical counterparts in these applications, owing to their high power density and their ability to be used in direct drive configurations.

Notwithstanding the advantages mentioned above, hydraulic servo systems are typically characterized by low damping, time-varying parameters, and nonlinear dynamics. These properties render high-performance control design challenging.

Typically linear controllers are designed based on a model of the system, which is linearized in a given operating point. However, typically the eigenfrequency of the hydraulic plant varies with the piston position, and the operation dependent nature of some of the parameters is not considered. This leads to the controller being conservatively tuned to achieve acceptable relative stability margins to account for the neglected dynamics and the uncertainty in the parameters.

Nonlinear control methods applied in hydraulic servo systems with symmetrical cylinders have been proven experimentally to provide increased tracking performance in Bech et al. (2013) and Andersen et al. (2015). This results from the design procedure, which considers the hydraulic system's nonlinear dynamics and time-varying parameters.

One method of designing control algorithms is the backstepping technique. Backstepping is directly ap-

doi:10.4173/mic.2023.1.3

plied to systems that are modelled by systems of equations in strict feedback form. Using the backstepping algorithm and by appropriately selecting the control variable, a Lyapunov function for the closed loop system is constructed, guaranteeing the boundedness of the states.

In the current paper, a novel simple backstepping controller is hence presented. The main focus is here on the stability of the system and minor on the performance, although both simulation and experimental results are presented and compared with those of some classic linear controllers.

1.1 State of the art

Owing to the aforementioned advantages, nonlinear controllers based on backstepping have been designed and applied to electro-hydraulic systems. Furthermore, different techniques have been applied alongside the backstepping design to account for the parameter variations.

1.1.1 Combination with adaptive techniques

In Ursu et al. (2006), a backstepping controller is designed for a symmetrical cylinder for force and position control. Simulation results are performed to compare the tracking performance of different controllers. In Liu and Alleyne (1999), a backstepping controller is designed for pressure tracking of a symmetrical electro-hydraulic actuator. Full state feedback is assumed. An adaptation algorithm based on the Lyapunov function has been designed to account for the lack of accurate knowledge of the valve's discharge coefficient. In the first part of Sirouspour and Salcudean (2000), exact backstepping controller design is applied to an asymmetric cylinder for position reference tracking, while in the second part, an adaptation algorithm for the estimation of the hydraulic parameters is established. This algorithm is based on the Lyapunov function. In the experimental results, the proposed controller, albeit complex, outperforms a PD controller. However, the mechanical system's parameters are assumed to be precisely known, and that full state feedback is available.

The problem of unknown mechanical and hydraulic parameters is solved in Kaddissi et al. (2007) by an identification procedure based on the recursive least squares algorithm. This procedure is realized before the control design with a sinusoidal input plus low power white noise. Afterward, the exact, full state backstepping algorithm is designed and compared with a PID controller. The nonlinear controller is found to require less control input power for better tracking performance, especially when the load is increased. The Lyapunov function is designed so that the state matrix of the resulting closed loop error dynamics is almost diagonal when the tuning parameters are selected appropriately. Then, the negative effects of the magnitude of the hydraulic elements are alleviated.

In Yao et al. (1999), the Adaptive Robust Control (ARC) method is applied to an asymmetrical cylinder. This method is based on backstepping, and for each step, the virtual control law is composed of adaptive and robust terms. In Yao et al. (2001), ARC is applied on a symmetrical cylinder. The discontinuous projection method is used alongside tuning functions for parameter estimation. Both uncertain parameters and uncertain nonlinearities are dealt with. The resulting controller is somewhat complex and many tuning parameters are required.

In all the previous works, the use of adaptive laws assumes that the system is linear in the parameters. However, this assumption does not hold when the initial control volumes are unknown. This is tackled in Guan and Pan (2008), where adaptive backstepping control is applied to a valve actuated asymmetrical cylinder. A modified Lyapunov function is introduced so that the uncertain initial volumes can be estimated and used for control design, even though the system is not linear in parameters regarding these terms. Furthermore, the overall controller is composed of many tuning parameters, which can be difficult to select. Experimental results show that the proposed controller provides superior tracking performance to a non-adaptive backstepping controller and to an adaptive controller assuming known initial control volumes. The same approach was applied to a pump controlled asymmetrical cylinder system in Ahn et al. (2014).

In Choux and Hovland (2010) and Choux (2011), an adaptive backstepping controller is designed for a symmetrical cylinder servo system. The tuning functions approach is used. Simulations show that including the valve's second-order dynamics increases tracking performance. The full state vector is considered available, and the resulting control law is complex and computationally heavy. This is deduced by the number of assignments and mathematical manipulations of the algorithm.

To overcome the increased complexity of the backstepping based controllers, mainly due to the differentiation of the virtual control laws, different approaches have been made. In Choux et al. (2012), the backstepping design stops at the first two steps, and the load pressure error is regulated by a PID controller. The simulation results, comparing the developed scheme to the one proposed in Choux and Hovland (2010) augmented with the LuGre friction model, present good tracking performance. The complexity of the control

algorithm is reduced by a wide margin. However, stability is not proven for the whole system, with or without including the valve dynamics. Another method, described in Schmidt (2012), is proposed to decrease the complexity. The system is a 1 DOF manipulator, actuated by an asymmetrical, servo valve controlled cylinder. An adaptive backstepping controller is designed similarly to Guan and Pan (2008). For the complexity to be reduced and ease of implementation, the final step in the backstepping procedure is omitted. The force controller is designed as a pressure feedback loop and a proportional controller. Furthermore, the backstepping controller for the mechanical part is reduced to a PD controller by noticing the resulting virtual control law of the second step. The overall tuning of the PD controller is based on linear techniques. The resulting controller presents increased end-point trajectory tracking performance compared to a linear reference controller with flow feedforward.

Instead of adapting to an unknown disturbance, such as the external force, a disturbance observer is utilized in Bakhshande and Sffker (2017). The observer also estimates the states of the system. The backstepping design procedure then follows. The controller is compared experimentally to a Sliding Mode Controller (SMC) and a proportional linear controller, showing increased tracking performance.

As mentioned above, a controller is designed using the backstepping algorithm in this paper. The focus is not on obtaining the most accurate tracking performance but on presenting a simple algorithm, where the increased complexity due to virtual control laws differentiation and the high number of tuning parameters for the adaptation laws, is avoided. This is hence achieved using a sliding mode disturbance observer. The benefit of the current algorithm is hence a robust controller with few tuning parameters, which may cope with the non-linearities encountered in hydraulic systems. Finally, the algorithm is experimentally validated and compared with that of classical linear controllers, showing that the performance of the backstepping controller is worse than that of the linear controllers for the considered trajectory. However, this is partly due to the conservatively designed backstepping controller and the limitations in the trajectory used, where the current paper focuses on proving the stability. Finally, recommendations for how the tracking performance may be improved are, however, given.

2 System Description - Modelling

In this section, the model of the system to be controlled is developed. The system is comprised of the load, which is the links of the manipulator in the different configurations, two symmetrical cylinders, and two servo valves that control the flow to the cylinders' chambers. An illustration of the manipulator is shown in Figure **??**. Initially, the dynamic model of the manipulator, denoted as the mechanical model, is derived. Then, the dynamic model of the actuators, denoted the hydraulic model, follows.

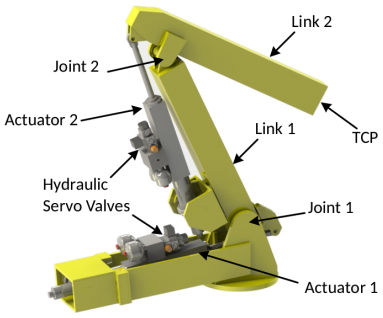

Figure 1: Illustration of the hydraulically actuated manipulator.

2.1 Mechanical model

Selecting the joint angles as generalized coordinates and under the assumption that the position of the centers of mass for each link-actuator combination does not vary depending on the piston position, the equations of motion are derived from the Euler-Lagrange equations as Spong and Vidyasagar (1989):

$$\mathbf{D}(\mathbf{q})\ddot{\mathbf{q}} + \bar{\mathbf{C}}(\mathbf{q}, \dot{\mathbf{q}})\dot{\mathbf{q}} + \bar{\mathbf{G}}(\mathbf{q}) = \boldsymbol{\tau} \tag{1}$$

where $\mathbf{q} = \begin{bmatrix}\phi_1 & \phi_2\end{bmatrix}^T$ is the vector of joint angles, $\mathbf{D}(\mathbf{q})$ is the inertia matrix, $\bar{\mathbf{C}}(\mathbf{q}, \dot{\mathbf{q}})\dot{\mathbf{q}}$ is the vector of Coriolis and centrifugal forces, $\bar{\mathbf{G}}(\mathbf{q})$ is the vector of gravitational forces and $\boldsymbol{\tau}$ is the vector of input joint torques. The mechanical model can be described in actuator space, i.e. with actuator lengths as coordinates using the law of cosines. The rate of changes of joint angles is related to the velocity of each piston via:

$$\dot{\mathbf{q}} = \mathbf{J}_s(\mathbf{x}_p)\dot{\mathbf{x}}_p \tag{2}$$

where $\mathbf{x} = \begin{bmatrix}x_{p_1} & x_{p_2}\end{bmatrix}^T$ is the vector of piston positions. It is more convenient to express the input vector in terms of the forces applied by the actuators instead of the torques applied to each link. This is achieved by the relationship:

$$\boldsymbol{\tau} = \mathbf{J}_s^T(\mathbf{x}_p)\mathbf{F} \tag{3}$$

As a result, the dynamic model of the manipulator can be expressed in terms of piston positions as:

$$\mathbf{M}(\mathbf{x}_p)\ddot{\mathbf{x}}_p + \mathbf{C}(\mathbf{x}_p, \dot{\mathbf{x}}_p)\dot{\mathbf{x}}_p + \mathbf{G}(\mathbf{x}_p) = \mathbf{F} \tag{4}$$

2.2 Hydraulic model

The motion of the piston of each actuator is describe the by Newton's second law:

$$m_p \ddot{x}_{p_i} = A(P_{A_i} - P_{B_i}) - B_v \dot{x}_{p_i} - F_C(\dot{x}_{p_i}) \quad (5)$$

where $i = 1, 2$ for each actuator. P_A, P_B denote the absolute pressure of the cylinders' chamber A and B respectively, B_v denotes the viscous friction coefficient and F_C the Coulomb friction. The pressure dynamics for each chamber are described via the flow continuity equation Jelali and Kroll (2002). Since the orifices of each servo valve are matched and symmetric and under the assumption that the effective oil bulk moduli in both chambers are equal, the load pressure $P_L = P_A - P_B$ is used as introduced so that the order of the system is reduced. Moreover, only internal leakage is considered between the chambers. This leakage flow is considered laminar. The flow continuity equation reduces to:

$$\dot{P}_{L_i} = \left[\frac{\beta_{eff}}{V_{A_i(x_{p_i})}} + \frac{\beta_{eff}}{V_{B_i(x_{p_i})}} \right] (-C_l P_{L_i} - A\dot{x}_{p_i} + Q_{L_i}) \quad (6)$$

where $V_{A,B}$ is the volume of each chamber of the cylinder plus the initial volume of the oil contained in the hoses and the valves. The flow through the orifices of the servo valves is assumed turbulent and is given by Jelali and Kroll (2002):

$$Q_L = K_v x_v \sqrt{\frac{P_s - P_t - \text{sign}(x_v) P_L}{2}} \quad (7)$$

where P_s, P_t are the supply and tank pressures respectively, x_v is the displacement of the valve's spool and K_v is the discharge coefficient of the valve's orifices. In (7), the sign(x_v) is defined as:

$$\text{sign}(x_v) = \begin{cases} 1 & x_v \geq 0 \\ -1 & x_v < 0 \end{cases}$$

One way to obtain a model that describes the dynamic properties of the spool position of the servo valve is via the frequency response, given in the valve's datasheet. The dynamics can be approached by those of a second order LTI system:

$$X_v(s) = \frac{\omega_v^2}{s^2 + 2\zeta_v \omega_v s + \omega_v^2} U_v(s) \quad (8)$$

However, the natural frequency of the servo valve is much higher than the frequency of operation of the actuators and as a result, the model of the servo valve is only considered in the simulation model. For the analysis, it is assumed that $x_v \approx u_v$.

The masses of the piston and the rod of each cylinder are considered negligible compared to the elements of the inertia matrix. Consequently, from (5), the force applied to each link from the respective actuator can be written as:

$$F_i = AP_{L_i} - B_v \dot{x}_i - F_C(\dot{x}_i) \quad (9)$$

2.3 Model of the system

In order to derive the system of differential equations that describe the whole manipulator and actuator system, (9) is substituted into (4):

$$\mathbf{M}(\mathbf{x}_p)\ddot{\mathbf{x}}_p + [\mathbf{C}(\mathbf{x}_p, \dot{\mathbf{x}}_p) + \mathbf{B}_v]\dot{\mathbf{x}}_p + \mathbf{G}(\mathbf{x}_p) + \mathbf{F}_C = \mathbf{A}\mathbf{P}_L \quad (10)$$

where $\mathbf{B}_v = diag(B_{v_i})_{2\times 2}$, $\mathbf{A} = diag(A_i)_{2\times 2}$, $\mathbf{F}_C = \begin{bmatrix} F_{C_1}(\dot{x}_{p_1}) & F_{C_2}(\dot{x}_{p_2}) \end{bmatrix}^T$ and $\mathbf{P}_L = \begin{bmatrix} P_{L_1} & P_{L_2} \end{bmatrix}^T$. The dynamics of the system are described by (10), (6) and (7).

3 Problem formulation

The objective of the design is that the tool centre of the manipulator tracks the desired trajectory. This trajectory is illustrated alongside the workspace of the manipulator in Figure 2. This trajectory has been designed using a seventh-order time polynomial so that the velocity, acceleration, and jerk at the starting and ending position of each segment are zero. The total completion time has been selected to be equal to 5 s. Through the inverse kinematics of the manipulator, the reference trajectory is expressed as piston position and velocities references for each hydraulic servo system.

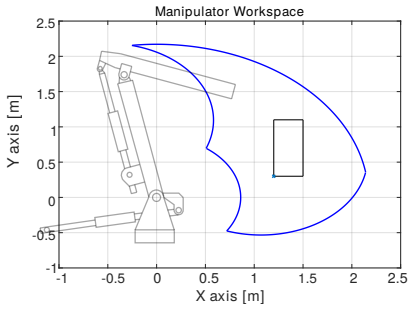

Figure 2: Desired tool center trajectory within the manipulator's workspace.

A fundamental problem in designing a control algorithm to achieve trajectory tracking is the uncertain and time-varying nature of the parameters. For example, the value of the effective oil bulk modulus is dependent on the oil temperature, the pressure of the

controlled volume as well as the free air trapped in the fluid. The last parameter is not easy to estimate, and the two former parameters vary during operation. Furthermore, the load attached to the tool center might also vary. Finally, depending on the reference velocity of the trajectory, the Coriolis terms can change.

In the case studied in this paper, the controllers are designed for each servo system separately. This leads to regarding each actuator-link combination as a SISO system. As a result, the model of each servo system is written from (10):

$$M_{ii}(\mathbf{x}_p)\ddot{x}_{p_i} + \left[C_{ii}(\mathbf{x}_p, \dot{\mathbf{x}}_p) + B_{v_i}\right]\dot{x}_{p_i} + G_i(\mathbf{x}_p) + \\ + F_{C_i}(\dot{x}_{p_i}) + M_{ij}(\mathbf{x}_p)\ddot{x}_{p_j} + C_{ij}(\mathbf{x}_p, \dot{\mathbf{x}}_p)\dot{x}_{p_j} = AP_{L_i} \quad (11)$$

with $i = 1, 2$ and $j = 2, 1$ for each servo system. In the following, the arguments i or j will be dropped, since the design is equivalent for both servo systems. The mechanical model can be written in state space form by selecting $x_1 = x_{p_i}$ and $x_2 = \dot{x}_{p_i}$:

$$\dot{x}_1 = x_2 \quad (12)$$

$$\dot{x}_2 = -\vartheta_1 x_2 - d(t) + \vartheta_2 P_{L_i} \quad (13)$$

$$\dot{P}_{L_i} = -\vartheta_3 P_{L_i} - \vartheta_4 x_2 + \vartheta_5 \bar{u}_i \quad (14)$$

where

$$\vartheta_1 = \frac{C_{ii} + B_{v_i}}{M_{ii}}, \quad \vartheta_2 = \frac{A}{M_{ii}}, \\ \vartheta_3 = \beta C_{l_i}, \quad \vartheta_4 = \beta A, \quad \vartheta_5 = \beta K_v, \quad (15) \\ \beta = \beta_{eff}\left[\frac{1}{V_A(x_{p_i})} + \frac{1}{V_B(x_{p_i})}\right] \\ d(t) = \frac{G_i + F_{C_i} + M_{ij}\ddot{x}_{p_j} + C_{ij}\dot{x}_{p_j}}{M_{ii}}$$

with $i = 1, 2$ and $j = 2, 1$ for each servo system. Furthermore, a pre-compensator has been used:

$$\bar{u}_i = u_{v_i}\sqrt{\frac{P_s - P_t - \text{sign}(u_{v_i})P_L}{2}}$$

In the following, the error between an estimated parameter and its actual value is defined as:

$$\tilde{\vartheta}_i = \hat{\vartheta}_i - \vartheta, \quad i = 1, ..4$$

4 Backstepping-based controller design

To proceed with the controller design, the error dynamics of the system to be stabilized are developed. The error variables are defined as:

$$z_1 = x_1 - r(t) \quad (16)$$

$$z_2 = x_2 - a_1 \quad (17)$$

$$z_3 = P_L - a_2 \quad (18)$$

where $r(t)$ is the position reference and $a_{1,2}$ are the desired values for the state variables x_2 and P_L respectively. The procedure for designing the control algorithm is presented in steps.

Step 1: The dynamics of the first error variable are written as:

$$\dot{z}_1 = \dot{x}_1 - \dot{r}(t) = z_2 + a_1 - \dot{r}(t) \quad (19)$$

In order to select a_1, a radially unbounded and decrescent function is selected as:

$$V_1(z_1) = \frac{1}{2}z_1^2 \quad (20)$$

whose time derivative becomes, using (19):

$$\dot{V}_1(z_1) = z_1\left[z_2 + a_1 - \dot{r}(t)\right] \quad (21)$$

The derivative of $V_1(z_1)$ can be rendered negative definite when $z_2 = 0$ by selecting a_1 as:

$$a_1(z_1) = -k_1 z_1 + \dot{r}(t) \qquad k_1 > 0 \quad (22)$$

Then

$$\dot{V}_1 = -k_1 z_1^2 = -2k_1 V_1 \quad (23)$$

and the origin is the Globally Exponentially Stable equilibrium point for z_1. Ensuring that $z_2 = 0$ is the objective of Step 2.

Step 2: The dynamics of the second error variable, using (18), can be written as:

$$\dot{z}_2 = -\vartheta_1 x_2 - d(t) + \vartheta_2 z_3 + \vartheta_2 a_2 - \dot{a}_1(z_1) \quad (24)$$

with $\dot{a}_1$ being exactly known. The variable a_2 is used as a virtual control input to drive z_2 to 0. Initially, to tackle the uncertainty in the input term, the virtual input variable is selected as Krstic et al. (1995):

$$a_2 = \hat{\rho}_2 u_2, \quad \hat{\rho}_2 = \frac{1}{\hat{\vartheta}_2} \quad (25)$$

Then, the system of the first two error state variables can be rewritten:

$$\dot{z}_1 = -k_1 z_1 + z_2 \quad (26)$$

$$\dot{z}_2 = \vartheta_2 z_3 - \vartheta_1 x_2 - d(t) - \dot{a}_1 + \vartheta_2\tilde{\rho}_2 u_2 + u_2 \quad (27)$$

where $\tilde{\rho}_2 = \hat{\rho}_2 - \rho_2$, with a decrescent and positive definite Lyapunov function candidate:

$$V_2 = V_1 + \frac{1}{2}z_2^2 + \frac{1}{2\gamma_1}\tilde{\vartheta}_1^2 + \frac{|\vartheta_2|}{2\gamma_2}\tilde{\rho}_2^2 \quad (28)$$

with time derivative:

$$\dot{V}_2 = -k_1 z_1^2 + z_2 \left[z_1 - \vartheta_1 x_2 + u_2 - d(t) - \dot{a}_1(z_1) \right] + \\ + \vartheta_2 z_2 z_3 + \frac{1}{\gamma_1} \tilde{\vartheta}_1 \dot{\tilde{\vartheta}}_1 + \tilde{\rho}_2 \left[\frac{|\vartheta_2|}{\gamma_2} \dot{\tilde{\rho}}_2 + z_2 \vartheta_2 u_2 \right] \tag{29}$$

This is under the assumption that the rate of change of ϑ_2 is much slower than the rate of adaptation of the parameter ρ_2.

This derivative can be rendered negative definite using the certainty equivalence virtual control input and parameter adaptation laws:

$$u_2 = -z_1 + \hat{\vartheta}_1 x_2 + u_{2r} + \dot{a}_1 - k_2 z_2, \qquad k_2 > 0 \tag{30}$$

$$\dot{\hat{\vartheta}}_1 = -\gamma_1 z_2 x_2 \tag{31}$$

$$\dot{\hat{\rho}}_2 = -\gamma_2 z_2 u_2 \tag{32}$$

under the assumption that the rate of variation of the uncertain parameters is much slower than the rate of adaptation and knowing the sign of parameter ϑ_2. The robust term u_{2r} is designed to tackle the time-varying uncertainty $d(t)$. In order to tackle the disturbance state dependent term $d(t)$, the robust input term u_{2r} can be selected as:

$$u_{2r} = -\frac{D}{\delta} z_2 \tag{33}$$

where D is the maximum absolute value of the disturbance term $d(t)$. This may be calculated using the desired trajectory data by pre-assuming stability. δ is a positive number, the value of which is a trade-off between having a large feedback gain and achieving z_1 and z_2 being close to the origin.

Using Eqs. (30) and (33), (29) may be written as:

$$\begin{aligned} \dot{V}_2 &= -k_1 z_1^2 - k_2 z_2^2 + \vartheta_2 z_2 z_3 + \left[-z_2^2 \frac{D}{\delta} - z_2 d(t) \right] \\ &= -k_1 z_1^2 - k_2 z_2^2 + \vartheta_2 z_2 z_3 - \frac{D}{\delta} \left(z_2 + \frac{\delta}{2D} d(t) \right)^2 + \\ &+ \frac{\delta}{4D} d(t)^2 \leq -k_1 z_1^2 - k_2 z_2^2 + \vartheta_2 z_2 z_3 + \frac{\delta}{4D} d(t)^2 \\ &\leq -k_0 \left(z_1^2 + z_2^2 \right) + \frac{\delta D}{4}, \qquad k_0 = \min\{k_1, k_2\} \end{aligned} \tag{34}$$

In the last inequality of Eq. (34), the cross term $\vartheta_2 z_2 z_3$ was neglected since the next step of the design ensures that z_3 goes to 0 as $t \to \infty$. Then, (34) is negative semi-definite in the set:

$$\mathcal{S} = \left\{ \mathbf{z} \in \mathbb{R}^2 : |\mathbf{z}| \geq \sqrt{\frac{\delta D}{4k_0}} \right\} \tag{35}$$

Outside the set, the state variables' trajectories diverge from the origin towards the surface of the circle with radius $\sqrt{\frac{\delta D}{4k_0}}$. When inside the set, the following holds:

$$\dot{V}_2 \leq Q(\mathbf{z}) \leq 0$$

$$Q(\mathbf{z}) = k_0 \left(z_1^2 + z_2^2 \right) - \frac{\delta D}{4}$$

By applying the LaSalle-Yoshizawa theorem, from Krstic et al. (1995), it can be shown that

$$\lim_{t \to \infty} Q(\mathbf{z}) = 0$$

and the state variables converge ultimately on the circumference of the circle with radius $\sqrt{\frac{\delta D}{4k_0}}$. Here, the trade-off in the selection of δ can be seen. The smaller the value of δ, the larger the magnitude of the robust term u_{2r} when $z_2 \neq 0$ but the radius of the circle where the states z_1 and z_2 converge becomes smaller. The state variables $\tilde{\rho}_2, \tilde{\vartheta}_1$ are proven to be bounded.

Step 3 The error dynamics of the system can be written:

$$\dot{z}_1 = -k_1 z_1 + z_2 \tag{36}$$

$$\dot{z}_2 = -z_1 - k_2 z_2 + \vartheta_2 z_3 + \tilde{\vartheta}_1 x_2 + \vartheta_2 \tilde{\rho}_2 u_2 + [u_{2r} - d(t)] \tag{37}$$

$$\dot{z}_3 = -\vartheta_3 P_L - \vartheta_4 x_2 + \vartheta_5 \bar{u} - \dot{a}_2 \tag{38}$$

The increased complexity of the backstepping algorithm, or explosion of terms, can be seen by the time derivative of a_2, which needs to be canceled. This would also introduce the need for acceleration feedback. Moreover, the three uncertain terms $\vartheta_{3,4,5}$ would need to be estimated, as well as ϑ_2 since no tuning functions were used in the previous step. These adaptation algorithms would require more gains to be adjusted. To avoid the increased complexity, the approach of the paper is the following. If $\bar{u}$ is selected as:

$$\bar{u} = \frac{1}{\bar{\vartheta}_5} u_3, \qquad \bar{\vartheta}_5 = \sqrt{|\vartheta_{5,min}||\vartheta_{5,max}|} \tag{39}$$

Equation (38) becomes:

$$\dot{z}_3 = \underbrace{-\vartheta_3 P_L - \vartheta_4 x_2 - \dot{a}_2 + \left(\frac{\vartheta_5}{\bar{\vartheta}_5} - 1 \right) u_3}_{g} + u_3 \tag{40}$$

A Lyapunov function candidate for the system is:

$$V_3 = V_2 + \frac{1}{2} z_3^2 \tag{41}$$

Its time derivative is shown in Eq. (42).

$$\dot{V}_3 \leq -k_1 z_1^2 - k_2 z_2^2 + \frac{\delta D}{4} + z_3 \left[\underbrace{\vartheta_2 z_2 - \vartheta_3 P_L - \vartheta_4 x_2 - \dot{a}_2 + \left(\frac{\vartheta_5}{\bar{\vartheta}_5} - 1 \right) u_3}_{g} + u_3 \right] \tag{42}$$

The control input u_3 can be selected as:

$$u_3 = -k_3 z_3 + u_{3r} + u_C, \qquad k_3 > 0 \tag{43}$$

where u_{3r} is a robust term to tackle the uncertainty stemming from the term $\vartheta_2 z_2$ and u_c is a term that is assumed to directly cancel the disturbance term g and will be designed in the following. The derivative of V_3 becomes:

$$\begin{aligned} \dot{V}_3 \leq & -k_1 z_1^2 - k_2 z_2^2 - k_3 z_3^2 + \frac{\delta D}{4} + \vartheta_2 z_2 z_3 + z_3 u_{3r} + \\ & + z_3 (g + u_c) \\ \leq & -k_1 z_1^2 - k_2 z_2^2 - k_3 z_3^2 + \frac{\delta D}{4} + \frac{\vartheta_{2,max}^2 z_2^2 z_3^2}{2\epsilon} + \\ & + \frac{\epsilon}{2} + z_3 u_{3r} + z_3 (g + u_c) \end{aligned} \tag{44}$$

which is valid for $\epsilon > 0$, and Young's inequality has been used. Selecting

$$u_{3r} = -z_3 \frac{\vartheta_{2,max}^2 z_2^2}{2\epsilon} \tag{45}$$

and assuming perfect cancellation of the disturbance term g by u_C,

$$\dot{V}_3 \leq -\min\{k_1, k_2, k_3\} |\mathbf{z}|^2 + \frac{\delta D + 2\epsilon}{4} \tag{46}$$

Applying the LaSalle-Yoshizawa theorem again can prove the boundedness of the state vector $\mathbf{z}$.

Design of the disturbance observer In order to select u_C in (43), a disturbance observer that directly cancels the term g in (40) is designed. Selecting a sliding surface S as:

$$S = z_3 + w \tag{47}$$

with time derivative, using (40), defined as:

$$\dot{S} = g + u_3 + \dot{w} \tag{48}$$

and w a function to be selected, the aim becomes to drive S and $\dot{S}$ to 0 in finite time. A radially unbounded Lyapunov function candidate for the surface S is:

$$V_S = \frac{1}{2} S^2 \tag{49}$$

Its time derivative along the solutions of (48) becomes:

$$\dot{V}_S = S (g + u_3 + \dot{w}) \leq |S| G + S (u_3 + \dot{w}) \tag{50}$$

The term G is considered as an upper bound of g and is selected in the following. If

$$\dot{w} = v_S - u_3 \tag{51}$$

and

$$v_S = -\rho \, \text{sign}(S) \tag{52}$$

then

$$\dot{V}_S \leq |S| G + S v_S \leq |S| (G - \rho) = -\frac{\alpha}{\sqrt{2}} |S| = -\alpha V_S^{1/2} \tag{53}$$

where $\rho = G + \frac{\alpha}{\sqrt{2}}$ and $\alpha > 0$ selected so that the desired reaching time for the sliding mode is achieved. Since in finite time:

$$\dot{S} = 0 \Rightarrow g + u_3 + \dot{w} = 0 \Rightarrow g + u_3 + u_{S,eq} - u_3 = 0 \Rightarrow \tag{54}$$

$$\Rightarrow u_{S,eq} = -g \tag{55}$$

a suitable selection for the term u_C is $u_{S,eq}$ because on the sliding surface directly cancels the disturbance g. This is achieved by low pass filtering the discontinuous signal u_S:

$$u_C = \frac{1}{\tau s + 1} \left[-\rho \, \text{sign}(S) \right] \tag{56}$$

The low pass filter time constant was set around five times lower than the sampling period, which was 5e-4 s.

Selection of the term G The upper bound of the term g, used in (50), is selected as:

$$\begin{aligned} G = & |\vartheta_3|_{max} |P_L| + |\vartheta_4|_{max} |x_2| + |\dot{\hat{\alpha}}_2| + \\ & + |\beta_5 - 1| K_3 |z_3| + |\beta_5 - 1| |u_3| \end{aligned} \tag{57}$$

where $\beta_5 = \sqrt{\frac{|\vartheta_{5,max}|}{|\vartheta_{5,min}|}}$. The direct measurements of the signal are used.

The estimation of the derivative of the second virtual control law, $\hat{\alpha}_2$, is acquired via a second order differentiation using the super twisting algorithm. It has been

assumed that the second derivative of α_2 is bounded, an assumption that pre-requires stability.

In order to evaluate the closed loop stability using the disturbance observer, the derivative of V_3 is re written:

$$\dot{V}_3 = -k_1 z_1^2 - k_2 z_2^2 - k_3 z_3^2 + \frac{\delta D}{4} + \frac{\epsilon}{2} + z_3 u_{res} \quad (58)$$

where u_{res} is a residual term stemming from the difference between u_C and u_S due to the low pass filter lag. In the case that the time constant of the filter is sufficiently small, it can be assumed that $u_C \approx u_S$, and the states $z_{1,2,3}$ are bounded.

The closed loop system and selection of the feedback gains $\mathbf{k_{1,2,3}}$ Assuming that $u_C \approx u_{S,eq}$, the closed loop system dynamics become:

$$\dot{\mathbf{z}} = \begin{bmatrix} \dot{z}_1 \\ \dot{z}_2 \\ \dot{z}_3 \end{bmatrix} = \mathbf{A}\mathbf{z} + \begin{bmatrix} 0 \\ 1 \\ 0 \end{bmatrix} \left(\tilde{\vartheta}_1 x_2 + \vartheta_2 \tilde{\rho}_2 u_2 \right) + \begin{bmatrix} 0 \\ -1 \\ 0 \end{bmatrix} d(t) \quad (59)$$

$$\mathbf{A} = \begin{bmatrix} -k_1 & 1 & 0 \\ -1 & -\left(k_2 + \frac{D}{\delta}\right) & \vartheta_2 \\ 0 & 0 & -\left(k_3 + \frac{\vartheta_{2,max}^2 z_2}{2\epsilon}\right) \end{bmatrix} \quad (60)$$

If the parameter estimation error and the disturbance term are neglected, the resulting nonlinear system can be investigated for its stability properties using Lyapunov analysis. This way, the choice of the gains $k_{1,2,3}$ can be facilitated so that stability of the closed loop system is preserved in the absence of disturbance terms.

Selecting as Lyapunov function candidate the positive definite function

$$W = \mathbf{z}^T \mathbf{z} \quad (61)$$

with time derivative :

$$\dot{W} = \mathbf{z}^T \left(\mathbf{A}^T + \mathbf{A} \right) \mathbf{z} \leq \lambda_{max} \left(\mathbf{A}^T + \mathbf{A} \right) \underbrace{\mathbf{z}^T \mathbf{z}}_{W} \quad (62)$$

The origin will be exponentially stable, in absence of any disturbances, if the real part of all the eigenvalues of $\mathbf{A}^T + \mathbf{A}$ is negative. It is also noted that the variable $\vartheta_2 = \frac{A}{M_{ii}(\mathbf{x_p})}$ is always positive and nonsingular. The eigenvalues can be calculated symbolically as:

$$\lambda_1 = -2k_1$$

$$\lambda_{2,3} = \frac{-\delta \vartheta_{2,max}^2 z_2^2 - [D + (k_2 + k_3)\,\delta]\,\epsilon \pm o}{\delta \epsilon}$$

$$o = \sqrt{\{\epsilon\,[\delta\,(k_2 - k_3) + D] - \delta z_2^2 \vartheta_{2,max}^2\}^2 + \vartheta_2^2 \delta^2 \epsilon^2}$$

The term o is always positive and real, since the term under the square root is always positive. As a result λ_3 is always negative for all values of z_2 and ϑ_2. Furthermore, since $k_1 > 0$, λ_1 is also negative. In order to render $\lambda_2 < 0$, its numerator is investigated. An initial approach is to select k_2 so that the positive term o is minimized. This happens when

$$k_2 = k_3 - \frac{D}{\delta} + \frac{z_2^2 \vartheta_{2,max}^2}{\epsilon} \quad (63)$$

Substituting (63) in the numerator of λ_2, it can be found that in order to be negative, the following should hold:

$$k_3 > \frac{\vartheta_2}{2} - \frac{z_2^2 \vartheta_{2,max}^2}{\epsilon} \quad (64)$$

or that $k_3 > \frac{\vartheta_{2,max}}{2}$ for robustness. It is also reminded that, since $k_3 > 0$, from (63) it can be deduced for k_3 that

$$k_3 > \frac{D}{\delta} > \frac{D}{\delta} - \frac{z_2^2 \vartheta_{2,max}^2}{\epsilon} \quad (65)$$

Since along the required trajectory the term $\frac{D}{\delta} > \frac{\vartheta_{2,max}}{2}$, it is decided that

$$k_2 = k_3 - \frac{D}{\delta} + \frac{z_2^2 \vartheta_{2,max}^2}{\epsilon}$$

$$k_3 > \frac{D}{\delta}$$

with the resulting eigenvalues being

$$\lambda_1 = -2k_1 \qquad \lambda_{2,3} < -\left(\vartheta_{2,max} \mp \vartheta_2\right) \quad (66)$$

5 Simulation results

To investigate the performance of the system with the presented controller, this has first been tested in a simulation model. Two linear controllers have, in this regard, also been designed for comparison purposes, namely a Proportional-Integral (PI) and Proportional-Lead (PLead) controller. For the second servo system, instead of a PLead controller, a simple proportional (P) controller has been designed, given that its bandwidth is sufficient to track the reference signal. As part of designing the linear controllers a static gain pressure feedback and a velocity feedforward term have been also implemented to augment the tracking performance. The pressure feedback significantly helps to increase the damping in the system, whereas the velocity feedforward helps to reduce the tracking errors. The gain crossover frequency for the linear controllers was selected based on the frequency content of the position reference trajectory signals for each servo system,

acquired using Fast Fourier Transform (FFT) analysis. The phase margin for each servo system was designed to be 50° with the linear compensators. The results of all three controllers for respectively the first and second servo system are shown in figures 3 and 4, in which the resulting errors are also shown. The results are for the predetermined trajectory, shown in figure 2, which is repeated three times.

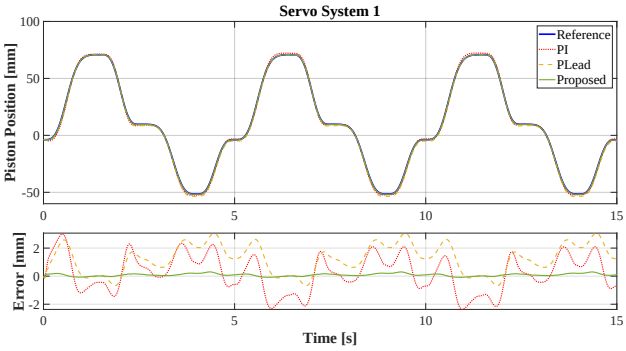

Figure 3: Simulated response for servo system 1, where the linear controllers are extended with a velocity feedforward.

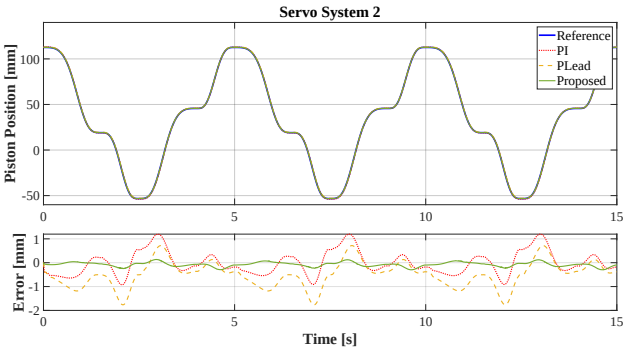

Figure 4: Simulated response for servo system 2, with velocity feedforward included with linear controllers.

From the above results it is seen that for both the first and second servo system the proposed controller outperforms the linear controllers. In both cases with errors which are below 1 mm in for all parts of the trajectory. Therefore the controller has also been experimentally tested as presented next.

6 Experimental results

The feasibility of the proposed control scheme was tested in the laboratory setup using cRIO hardware and the LabVIEW programming language. For the proposed control algorithm velocity measurements are needed, however, only a position sensor was available. As a result, a velocity observer was designed as a sliding mode differentiator, using the super twisting algorithm. Assuming boundedness of the states, the upper bound of the acceleration could be estimated beforehand, using the inverse kinematics of the manipulator and the trajectory data. The experimentally measured tracking performance of each servo system is presented in figures 5 and 6 for the proposed and the comparison control schemes.

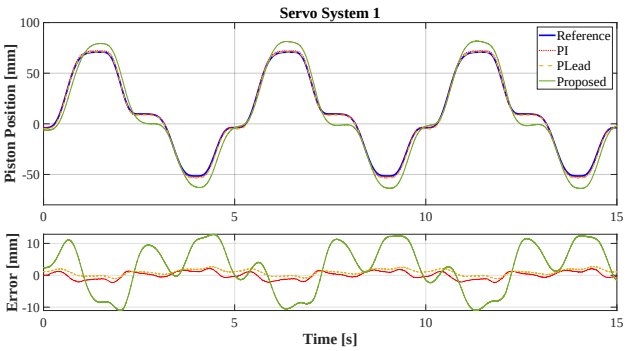

Figure 5: Tracking performance comparison of the proposed and reference controllers for servo system 1.

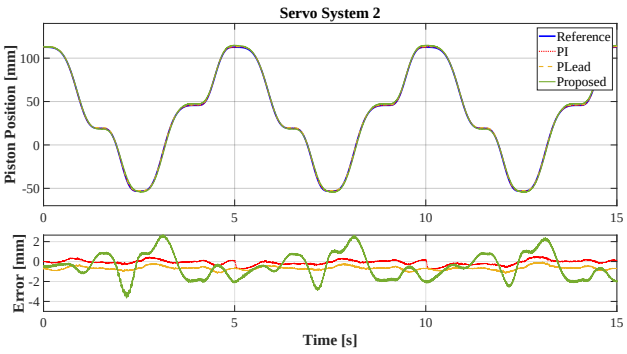

Figure 6: Tracking performance comparison of the proposed and reference controllers for servo system 2.

Initially, it can be seen that for the first servo system, the tracking performance of the linear controllers is significantly better compared to the proposed controller, unlike what was seen in the simulations. This is partly attributed the sliding mode differentiator, which, although also implemented in the simulation results, do have to account for measurement noise in the physical system. Secondly it is attributed the to the conservative settings of the gains $k_{1,2,3}$ that have been selected. Hence, increasing these gains while still pre-

serving closed loop stability, the tracking performance will be increased. As described before, the main focus of the paper is however not obtaining the best tracking performance, but on proving the stability of the presented algorithm, why the same parameters as used in the simulations are used.

To test the robustness of the proposed algorithm against parameter changes or disturbances, a change in the trajectory was introduced. The completion time was changed from 5 s to 3.5 s. As a result, the disturbance terms due to the cross-couplings of the two servo system will be increased, as well as the Coriolis terms. The tracking performance results for the faster trajectory are illustrated in Figures 7 and 8.

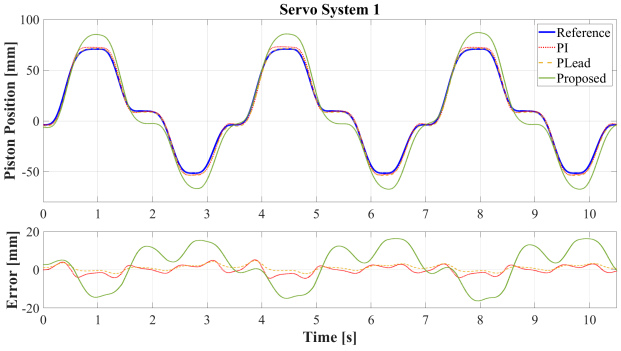

Figure 7: Tracking performance comparison of the proposed and reference controllers for servo system 1, faster trajectory.

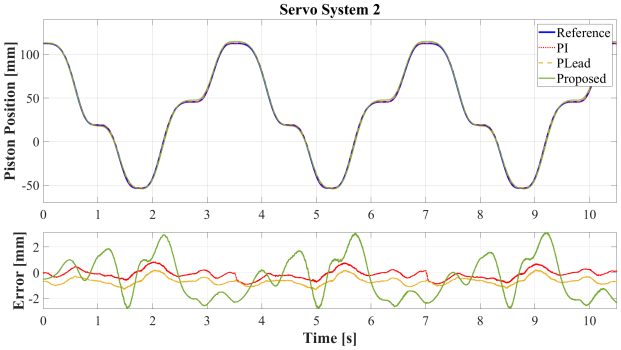

Figure 8: Tracking performance comparison of the proposed and reference controllers for servo system 2, faster trajectory.

Especially for the first servo system, a degradation of the tracking performance for the linear controllers is visible. For the second servo system, this is not easy to discern from Figure 8 alone. Due to the already wide bandwidth of the second servo system, the specific trajectory can be tracked using only the P controller, even for the faster completion time. This can be easily interpreted from an FFT analysis of the piston position reference trajectory.

In order to quantify the performance degradation and the robustness of the proposed algorithm, different indexes can be selected to compare. A selection of these indexes is discussed in Mattila et al. (2017). In this article, the indexes that will be compared are the following:

$$e_{max} = max|e| = max|x_p - r|$$
$$e_{RMS} = \sqrt{\frac{1}{n}e^2}$$

where n is the number of samples. These indices, alongside their percent change due to the modified trajectory are presented in Table 1.

An initial observation can be made regarding the second servo system regarding the performance of the P controller. It can be seen that the performance of the P controller does not degrade by a wide margin and its tracking performance is satisfactory. This happens due to the selected trajectory and the implementation of the pressure feedback and velocity feedforward terms. Its frequency content, even for the faster completion time, lies in frequencies below a gain crossover frequency easily attainable by the use of pressure feedback and a simple gain. Furthermore, the PI controller suffers from the introduction of the integrator and this gain crossover frequency is decreased. Nonetheless, regarding the comparison controllers, the use of feedforward can achieve satisfactory tracking results, especially for the case where no integrator is included in the controller.

The robustness of the proposed algorithm lies in the sliding mode observer and the adaptation term of Eq. (25). Even though the tracking performance cannot be compared to that of the linear controllers, the tuning of the gains $k_{1,2,3}$ has been conservative. Other choices that could increase the performance are:

- Choice of adaptation gains in Eqs. (31) and (32). Different adaptation algorithms could also be used by modifying the stability analysis accordingly.
- Selecting a smaller value for the variable δ of Eq. (33). According to the analysis using the quadratic Lyapunov function V_2 with time derivative shown in Eq. (34), the error states $z_{1,2}$ will be bounded on an ellipse closer to the origin. However large δ can lead to large control signal and saturate the valve. The same holds for the variable ϵ of Eq. (45).
- Selection of α and G, which consequently affect ρ in Eq. (52). A larger value for α leads to the disturbance term g in Eq. (40) being estimated

Table 1: Error indexes and percent increase for both servo systems

	e_{max} [mm]			e_{RMS} [mm]		
	$t = 5$ [s]	$t = 3.5$ [s]	$\uparrow$ %	$t = 5$ [s]	$t = 3.5$ [s]	$\uparrow$ %
Servo system 1						
PI	2.2803	4.2787	87.63	1.1621	1.9413	67.05
P-Lead	2.6390	3.1855	20.70	1.3170	1.6347	24.12
Proposed	12.8727	16.4203	27.56	7.7526	10.1904	31.44
Servo system 2						
PI	0.7548	0.8589	13.79	0.2526	0.3343	32.34
P	1.2209	1.2767	4.57	0.6770	0.6857	1.28
Proposed	3.1444	3.6404	13.62	1.3661	1.6234	18.83

and cancelled faster. The term G can be estimated in a less conservative way, leading to smaller $u_{S,eq}$ values, where the low pass filter time constant can be smaller.

7 Conclusion and future research

The purpose of this article was to investigate whether the complexity of the backstepping control technique may be simplified in terms of the complexity due to the increasing amount of terms and virtual input derivatives. This was approached using sliding mode theory, using a disturbance observer in the last step of the backstepping algorithm. The result is the avoidance of over-parameterization, at least partially, without the use of tuning functions and also the use of a control law that is not of high complexity. The resulting closed loop system is bounded under specific assumptions, while the application to the laboratory system was straightforward. Trajectory tracking was performed without fine tuning a large number of parameters. Since the backstepping algorithm is intuitive in nature and can take into consideration the dynamics of the actuators, future research can focus on proving tighter stability margins for this algorithm including the dynamics of the low pass filter, as well as examining whether performance similar to the reference linear controllers can be achieved by increasing the state feedback gains and implementing different adaptation schemes.

References

Ahn, K. K., Nam, D. N. C., and Jin, M. Adaptive backstepping control of an electrohydraulic actuator. *IEEE/ASME Transactions on Mechatronics*, 2014. 19(3):987–995. doi:10.1109/TMECH.2013.2265312.

Andersen, T., Pedersen, H., Bech, M., and Schmidt, L. A low order adaptive control scheme for hydraulic servo systems. In *2015 International Conference on Fluid Power and Mechatronics (FPM)*. Harbin, China, pages 1148–1152, 2015.

Bakhshande, F. and Sffker, D. Robust control approach for a hydraulic differential cylinder system using a proportional-integral-observer-based backstepping control. In *2017 American Control Conference (ACC)*. Seattle, WA, USA, pages 3102–3107, 2017.

Bech, M. M., Andersen, T. O., Pedersen, H. C., and Schmidt, L. Experimental evaluation of control strategies for hydraulic servo robot. In *2013 IEEE International Conference on Mechatronics and Automation*. Takamatsu, Japan, pages 342–347, 2013.

Choux, M. *Nonlinear, Adaptive and Fault-tolerant Control for Electro-hydraulic Servo Systems*. Ph.D. thesis, Technical University of Denmark, 2011.

Choux, M. and Hovland, G. Adaptive backstepping control of nonlinear hydraulic-mechanical system including valve dynamics. *Modeling Identification and Control - MODEL IDENT CONTR*, 2010. 31(1):35–44. doi:10.4173/mic.2010.1.3.

Choux, M., Hovland, G., and Blanke, M. Cascade controller including backstepping for hydraulic-mechanical systems. *IFAC Proceedings Volumes*,

2012. 45(8):310–315. doi:10.3182/20120531-2-NO-4020.00046.

Guan, C. and Pan, S. Nonlinear adaptive robust control of single-rod electro-hydraulic actuator with unknown nonlinear parameters. *IEEE Transactions on Control Systems Technology*, 2008. 16(3):434–445. doi:10.1109/TCST.2007.908195.

Jelali, M. and Kroll, A. *Hydraulic Servo-systems: Modelling, Identification and Control*. Springer London, 2002.

Kaddissi, C., Kenne, J. P., and Saad, M. Identification and real-time control of an electrohydraulic servo system based on nonlinear backstepping. *IEEE/ASME Transactions on Mechatronics*, 2007. 12(1):12–22. doi:10.1109/TMECH.2006.886190.

Krstic, M., Kokotovic, P. V., and Kanellakopoulos, I. *Nonlinear and Adaptive Control Design*. John Wiley & Sons, Inc., 1995.

Liu, R. and Alleyne, A. Nonlinear force/pressure tracking of an electro-hydraulic actuator. *IFAC Proceedings Volumes*, 1999. 32(2):952–957. doi:10.1016/S1474-6670(17)56160-1.

Mattila, J., Koivumki, J., G. Caldwell, D., and Semini, C. A survey on control of hydraulic robotic manipulators with projection to future trends. *IEEE/ASME Transactions on Mechatronics*, 2017. 22:669–680. doi:10.1109/TMECH.2017.2668604.

Schmidt, T. *Adaptiv Backstepping Kontrol af Asymmetrisk Elektro-Hydraulisk System*. Master's thesis, Aalborg University, 2012.

Sirouspour, M. R. and Salcudean, S. E. On the nonlinear control of hydraulic servo-systems. In *Proceedings 2000 ICRA. Millennium Conference. IEEE International Conference on Robotics and Automation. Symposia Proceedings (Cat. No.00CH37065)*. San Francisco, CA, USA, pages 1276–1282 vol.2, 2000.

Spong, M. and Vidyasagar, M. *Robot Dynamics And Control*. Wiley, 1989.

Ursu, I., Ursu, F., and Popescu, F. Backstepping design for controlling electrohydraulic servos. *Journal of the Franklin Institute*, 2006. 343(1):94–110. doi:10.1016/j.jfranklin.2005.09.003.

Yao, B., Bu, F., and Chiu, G. T. C. Non-linear adaptive robust control of electro-hydraulic systems driven by double-rod actuators. *International Journal of Control*, 2001. 74(8):761–775. doi:10.1080/002071700110037515.

Yao, B., Bu, F., Reedy, J., and Chiu, G. T. C. Adaptive robust motion control of single-rod hydraulic actuators: Theory and experiments. In *Proceedings of the 1999 American Control Conference (Cat. No. 99CH36251)*. San Diego, CA, USA, pages 759–763 vol.2, 1999.